TRANSACTIONS OF THE INSTITUTE OF MEASUREMENT & CONTROL

Transactions of the Institute of Measurement and Control
0(0) 1–14

DOI: 10.1177/0142331212451991
tim.sagepub.com
SAGE

A new approach for measurement of pitch, roll and yaw angles based on a circular feature

Lei Liu and Zhimin Zhao

Abstract

This paper presents a simple, yet very effective approach to measure the three types of rotation angles by the method of imaging analysis. This approach is suitable for many actual applications, such as head pose tracking, vehicle monitoring, robotic operation, etc. In this paper, a circular feature is fixed on the object, which can do the rotational motion. By measuring the rotational angles of the circular feature based on perspective projection, we can obtain the object's rotational angles. We deduce the computation methods of the pure pitch, roll and yaw angles. Then we propose the methods of computing the pitch, roll and yaw angles in complex situations, which are different from the computation methods of pure pitch, roll and yaw angles. Based on the approach proposed in this paper, some experiments are conducted and the results show that the approach can achieve good performance when the rotation angles are in the scope of $\pm 90°$.

Keywords

Pitch, roll and yaw angles, computation method, circular feature, perspective projection

Introduction

An object's position and orientation in 3D space has been the focus of research in recent years (Beaudot and Mullen, 2006; Fantoni, 2008; Lu and Leinonen, 2005; Price and Morrison, 2009; Regan, 1989; Triggs, 2004). In 3D space, a change in the position of a rigid body is complicated to describe. It can be regarded as a combination of two distinct types of motion: translational motion and rotational motion. Translational motion occurs when every particle of the body has the same instantaneous velocity as every other particle, while rotational motion occurs if every particle in the body moves in a circle about a single line. This line is called the axis of rotation. In general, any rotation can be specified completely by the three angular displacements with respect to the rectangular co-ordinate axes x, y and z. Any change in the position of the rigid body can be completely described by three translational and three rotational co-ordinates.

Rotational motion is a more complicate movement than translational motion (Kremmer and Favier, 2000; Salgado et al., 2010). The motion of pitch, roll and yaw are three representative types of rotational motion. It has been found that the three types of motion have played significant roles in many scientific and engineering fields. In the field of computer vision, the motion of pitch, roll and yaw are often used to describe an object's rotational motion (Ji, 2002; Romero and Bobick, 2004; Zhu and Ji, 2004). In the field of human–machine interactions, understanding the user's focus of attention is critical for a variety of human–machine interactions, and head orientation is a key component for assessing gaze and attention focus. Head orientation can be specified given three rotational parameters: roll, pitch and yaw. Yaw motion, which is the most important rotation of the head, was studied (Romero and Bobick, 2004). Three types of rotational motion were also studied and three types of rotation angles generated in the process of the motion were estimated when solving the problem of head orientation (Ji, 2002). Yaw and pitch were studied when solving the problem of real-time face tracking (Zhu and Ji, 2004).

In the fields of aeronautics and astronautics, the motion of pitch, roll and yaw, which could represent the aircraft's orientation, were also studied (Kumar and Kumar, 1999; Shang and Palmer, 2011). We could obtain the flight attitude by the study on the three kinds of rotational motion. This motion has also been found in the research on vehicles (Dornaika and Sappa, 2009; Qiu and Griffin, 2005; Sappa et al., 2006). When a car moves along a road, it will also generate other motion in the car except the forward motion, as we can feel the car's shaking. The car's motion of yaw, pitch and roll were studied for the transmission of roll, pitch and yaw vibration to the backrest of a seat supported on a non-rigid car floor (Qiu and Griffin, 2005).

In the field of shipping, research on the motion of the ship, especially the motion of roll and yaw, are significant for the

College of Science, Nanjing University of Aeronautics and Astronautics, Nanjing, P. R. China

Corresponding author:
Zhimin Zhao, College of Science, Nanjing University of Aeronautics and Astronautics, Nanjing, P. R. China
Email: nuaazhzhm@126.com

safety of ship (Das and Das, 2005). The three angles were also used in the field of orthodontic diagnosis and treatment planning (Ackerman et al., 2007). Three rotational descriptors (pitch, roll and yaw) were used to supplement the planar terms (anteroposterior, transverse and vertical) in describing the orientation of the line of occlusion and the aesthetic line of the dentition. They were also used in patient positioning (Kaiser et al., 2006).

In industrial activities such as manufacturing and inspection, physical quantities like angle and length are benchmark parameters for maintaining and improving the quality of products. Conventionally, the measurement of pitch and yaw angles is based on the laser autocollimation method (Ennos and Virdee, 1982). A fundamental concept of this method is to magnify the angle changes as an optical magnifier, which consists essentially of a thin collimate laser beam projected onto the target plane reflector along the reflector surface normal, an objective lens receiving the reflected beam and a position-sensing detector located at the focal position of the objective lens. The small angular displacement of the target reflector is converted into linear displacement of the light spot on the focal plane by using the objective lens as the optical magnifier. The pitch and yaw angles can be detected simultaneously by using a two-axis position-sensing detector such as a quadrant photodiode. However, the conventional laser autocollimation method cannot detect the roll angle (Saito et al., 2009).

There has been much research on the method for calculating the pitch, roll and yaw angles. Though the three angles had been measured, the process was sophisticated and the methods were limited in special situations. There is considerable measurement error and the precision could not meet the requirement. So in this paper, we propose a new approach to imaging analysis based on a circular feature, which has many advantages, such as easy operability, simplicity, low cost and high precision.

The research introduced in this paper is a part of a research study on a head pose tracking system, which can measure the three angles (pitch, roll and yaw angles) relative to its original pose in real time. In this system, we take the feature-based approach in which a circular feature labelled with one or two diameters is fixed on a person's head. The object tracked by camera is the circular feature instead of the head. The research in this paper is fundamental for the circular feature's rotational motion.

Camera calibration is a necessary procedure in traditional photogrammetry, but the creativity in this paper is that the approach proposed does not need the complicated procedure of camera calibration. The only thing we should do is to compute the effective focal length of the camera, and set the initial position and orientation of the camera and the circular feature.

The remainder of this paper is structured as follows: next, we describe the definition of the three angles and the principle of the approach for estimation of the object's rotational angles during the motion of pitch, roll and yaw using a circular feature. Then the computation methods of the pure pitch, roll and yaw angles are described, followed by the computation methods for the pitch, roll and yaw angles in a complex situation. We present some experiments and discuss the results, and finally, the conclusions are given.

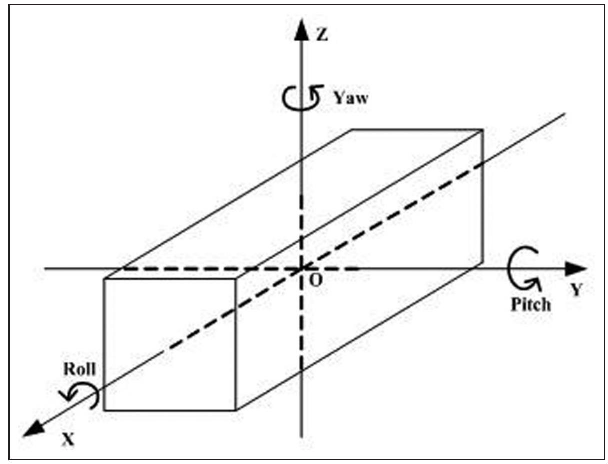

Figure 1 The motion of pitch, roll and yaw.

The principle of the approach

The pitch, roll and yaw angles

As a specification of a rotation obtained by applying three consecutive principal rotations, the Euler angle representation of a rotation or orientation is important, in part because most inertial systems produce Euler angles as outputs. In addition, Euler angles are often used to determine orientation in control mechanisms such as robotic arms and motion platforms.

There are 12 distinct ways to select a sequence of three principal axes and apply the principal rotations. Each ordered selection is a Euler angle convention. There are numerous conventions for Euler angles in use and many are named inconsistently. The two common used conventions are Z–X–Z convention (also known as the 3–1–3 convention) and X–Y–Z convention (also known as the 1–2–3 convention).

The Euler angles in the Z–X–Z convention are the three angles: α, β and γ. In some literature, α is called spin angle, β is called the nutation angle and γ is called the precession angle. These three angles specify a rotation as consecutive principal rotations using the Z-axis, the X-axis and the Z-axis again. The first principal rotation is about the Z-axis through angle α, followed by the X-axis through angle β, followed by the X-axis again through angle γ.

The Euler angles in the X–Y–Z convention are variously called Tait–Bryan angles, Cardano angles or nautical angles. There are three angles: ϕ, θ and ψ. ϕ is called the roll angle, θ is called pitch angle and ψ is called the yaw angle. These three angles specify a rotation as principal rotations about the space-fixed principal axes. The first rotation is by angle ψ about the Z-axis. The second is by angle θ about the Y-axis. The third is by angle ϕ about the X-axis.

Figure 1 shows a model of cubic box for introduction of the motion of pitch, roll and yaw. We consider a right handed co-ordinate system (X, Y, Z) with the origin point O.

The three types of rotational motion can be defined as follows: the yaw motion is the object's rotational motion about the Z-axis, the pitch motion is the object's rotational motion about the Y-axis and the roll motion is the object's rotational motion about the X-axis. We can set anticlockwise direction

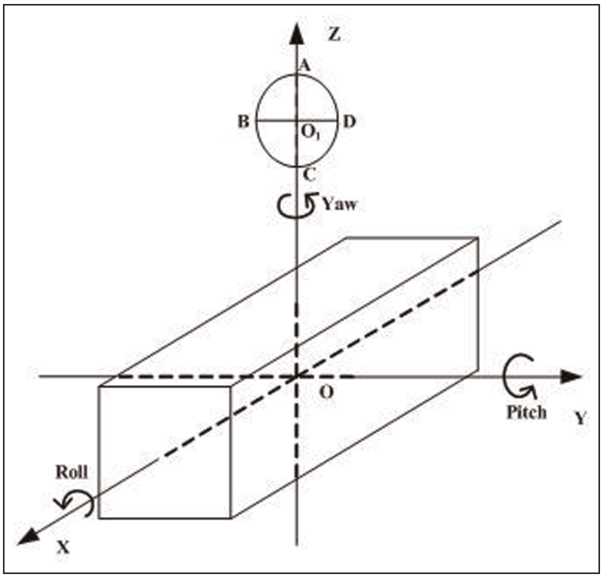

Figure 2 A circular feature is fixed on the object.

as the motion's positive direction from the view of facing on the positive direction of the three axes.

Method of imaging analysis

Based on the principle of computer vision and image processing, imaging analysis has been a popular method in many fields such as real-time measurement, pose estimation, and so on. There exist two common approaches to the solution of motion-image processing and recognition problems using the method of imaging analysis: the feature-based approach and the optical-flow approach. The feature-based approach (Cosar and Çetin, 2011; Han and Requicha, 1997; Shapiro and Brady, 1992) requires that correspondence be established between a set of features extracted from one image and those extracted from the next image. Various features have been adopted to establish such correspondence, including points, lines, planes and conics, and combination of these features (Ma, 1993; Tissainayagam and Suter, 2005). Amongst the available features, as a good candidate for object recognition, a circular feature has been widely applied and has been the focus of research.

How does one track the object's rotational motion and measure some parameters such as angles of rotational motion? The object can be a boat, a ship, a car or an aircraft, from which we can hardly find a similar feature. So we propose a general method wherein a circular feature is fixed on the object, and the model can be shown in Figure 2.

Figure 2 shows a circular feature, a circle O_1, which is set in the plane YOZ, is fixed on the object by a thin stick. The point O_1 is on the Z-axis. BD is a diameter that is parallel to the Y-axis, while AC is another diameter that is on the Z-axis. We can set a camera, which can take the images of the circular feature in front of the circular feature. When the object moves, no matter whether it is the motion of pitch, roll or yaw, the circular feature also does the same motion. So we can obtain the object's parameters of motion by measuring the circular feature's parameters of motion.

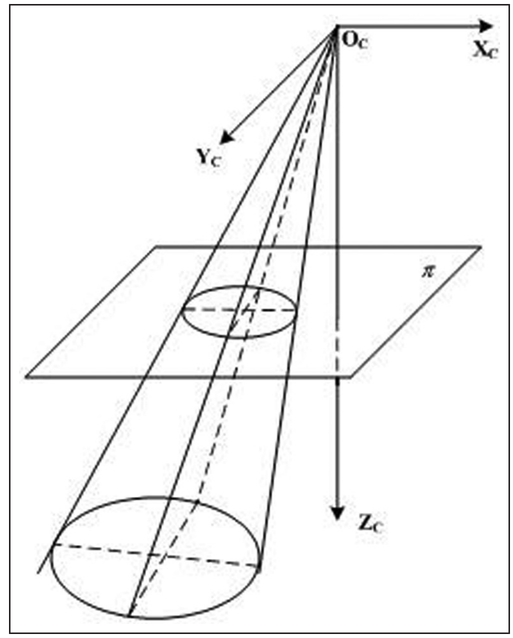

Figure 3 Perspective projection of a circular feature.

The perspective projection of a circular feature

The camera used to capture a sequence of images of circular feature is modelled as a pinhole camera with perspective projection. Perspective projection, also called the pinhole imaging model, is simple and practical. It is an ideal model based on the linear projection theory.

Figure 3 shows the perspective projection of a circular feature. There is a cone formed by the projection centre O_C as the vertex and every point on the circle in 3D space. The intersection of the cone and the image plane is the perspective projection of the circular feature, which is always an ellipse. When the circular feature's supporting plane is parallel to the image plane, the perspective projection of a circular feature is a circle, a special case of ellipse.

Computation methods of angles of pure pitch, roll and yaw

We can measure the object's rotation angles by measuring the circular feature's rotation angels, as we have mentioned in the previous section. In this section, we only consider the measurement of angles of pure pitch, roll and yaw. That is to say that there is only one kind of rotational motion each time. In most situations, the object's rotation angles are relatively small. So we only consider $\pm 90°$ as the scope of rotation angle in this paper, and our method proposed is also suitable for this situation.

Pitch angle

As we can see in Figure 2, when the object rotates about the Y-axis in the co-ordinate frame O–XYZ, the circle will do the same motion, which is called pitch motion.

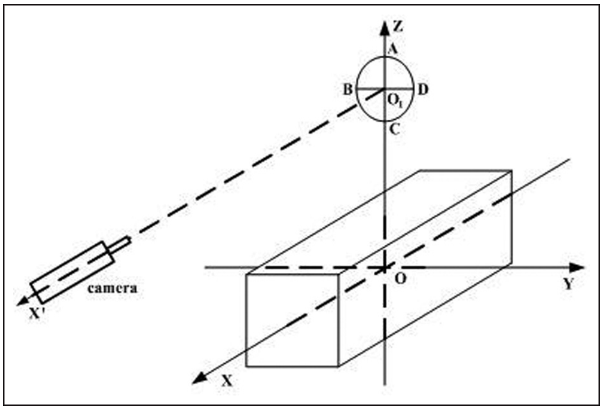

Figure 4 The schematic of measuring the angles of pitch, roll and yaw.

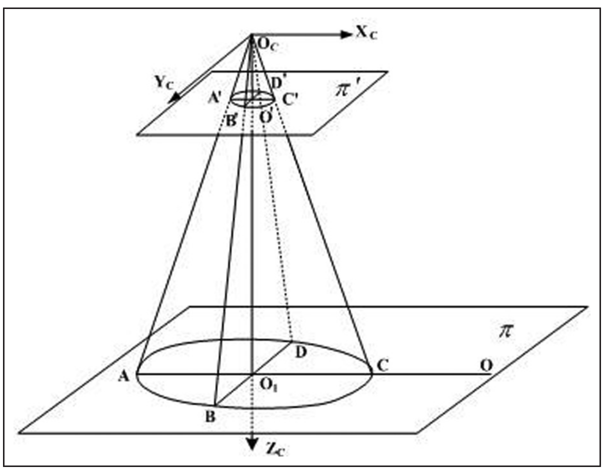

Figure 5 Perspective projection of the circular feature in initial status.

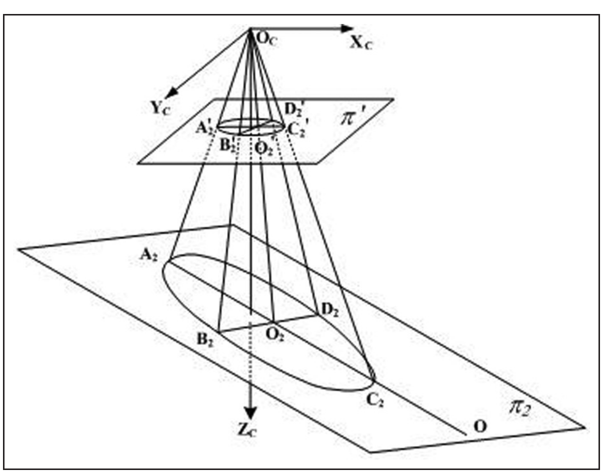

Figure 6 Perspective projection of the circular feature after the pitch motion.

We can take the images of the circular feature using a camera, which can be placed in front of the circle O_1. The

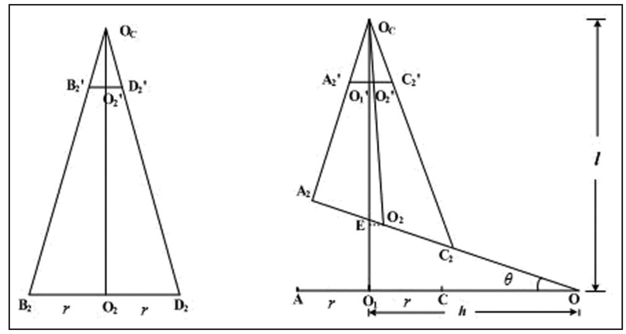

Figure 7 The simplified schematic representation of Figure 6.

optical axis of the camera should be perpendicular with the plane YOZ and pass the circle centre O_1 for the convenience of computation, as shown in Figure 4. The following analysis is under a premise that the circular feature can be completely imaged in the camera. The imaging of the circular feature based on perspective projection can be shown in Figure 5.

In Figure 5, a circle O_1, which lies in the plane π, has its perspective projection, a circle O' in the image plane π'. O_C–$X_C Y_C Z_C$ is the camera co-ordinate frame, in which O_C is the optic centre of the camera and the Z_C axis is perpendicular to the two planes π and π'. In Figure 6, the circle O_2, which is also the abovementioned circle O_1 but is in the position after a pitch motion, has its perspective projection, an ellipse O_2' in the image plane π'.

Based on geometrical reasoning, it can be shown that Figure 6 can be simplified schematically to Figure 7. Figure 7(a) and (b) display the triangle $\Delta O_C B_2 D_2$ and $\Delta O_C A_2 C_2$ separately. The pitch angle is θ. The distance between the optical centre O_C and the circle centre O_1 is l. The distance from O to O_1 is h. The radius of the circle O_1 is r.

For the convenience of computation, we should draw auxiliary line in Figure 7(b). From the point O_2, we draw the vertical line to the segment $O_C O_1$ and the foot point is E. In Figure 7(b), the segment AC moves to the segment A_2C_2 after the pitch motion. $A_2'C_2'$ is an axis of the image ellipse O_2'. We can obtain the equation as follows:

$$\frac{O_cO_2'}{O_cO_2} = \frac{O_cO_1'}{O_cE} \tag{1}$$

where $O_cE = O_cO_1 - EO_1 = l - h\sin\theta$. l is the distance between the optical centre O_C and the circle centre O_1 in initial status; h is the distance between the circle centre and the origin of the O–XYZ co-ordinate frame and θ is the pitch angle. The length of O_CO_1' is the camera's effective focal length f_0. In Figure 7(a), there is the following relationship:

$$\frac{O_cO_2'}{O_cO_2} = \frac{B_2'D_2'}{B_2D_2} \tag{2}$$

where $B_2'D_2'$ is another axis of image ellipse O_2'. We can set a as the length of the segment $B_2'D_2'$. Based on Equations (1) and (2), it can be shown that

$$\frac{O_cO'_1}{O_cE} = \frac{B'_2D'_2}{B_2D_2} \tag{3}$$

In Equation (3), $O_CO'_1$ represents the camera's effective focal length f_0. $O_cE = l - h\sin\theta$. The length of $B'_2D'_2$ is a. B_2D_2 is the diameter of the circle and the length is $2r$. So, the Equation (3) can also be shown as:

$$\frac{f_0}{l - h\sin\theta} = \frac{a}{2r} \tag{4}$$

So we can obtain the equation of the pitch angle.

$$\theta = \arcsin\frac{al - 2f_0r}{ah} \tag{5}$$

From Equation (5), we obtain the method for computing the pitch angle. We should know the values of five parameters: r, h, l, f_0 and a. The values of r (the radius of the circular feature), h (the distance between the circle centre and the origin of the O–XYZ co-ordinate frame) and l (the distance between the optical centre of the camera and the circle centre in initial status), can be measured on the scene. The values of f_0 (the effective focal length of the camera) can be calculated by acquiring an image of a known-size object. The value of a can be estimated from the acquired image. When the values of pitch angles increase, the direction of the pitch motion is positive.

Roll angle

As we can see in Figure 2, when the object rotates about the X-axis in the co-ordinate frame O–XYZ, the circle O_1 will do the same motion, which is called roll motion.

From the Figure 5, we can see that the segment BD is parallel with its projection B′D′ in the image plane. When the circle O_1 rotates about the point O, the two segments, BD and B′D′, always keep parallel. The simplified image of the circle O_1 can be shown in Figure 8. Obviously, we can obtain the method for computing roll angle ϕ by measuring the slope of the diameter B′D′.

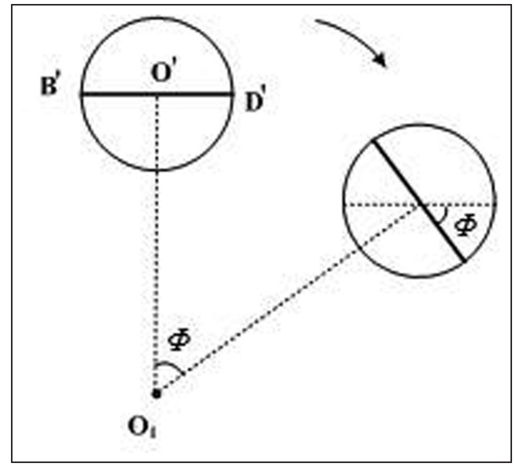

Figure 8 The image of the circle before and after the roll motion.

$$\phi = \arctan k_{BD} \tag{6}$$

where k_{BD} is the slope of B′D′, which is the image of diameter BD. When the values of roll angles increase, the direction of the roll motion is positive.

Yaw angle

As we can see in Figure 2, when the object rotates about the Z-axis in the co-ordinate frame O–XYZ, the circle O′ will do the same motion, which is called yaw motion.

As shown in Figure 5, the diameter BD has its perspective projection B′D′. Figure 9 is the perspective projection of the circle O_1 in Figure 5 after a yaw motion. We can see that the diameter BD of the circle has rotated to the position of B_1D_1 and the plane that the circle lies on is π_1, while the image plane is still π'.

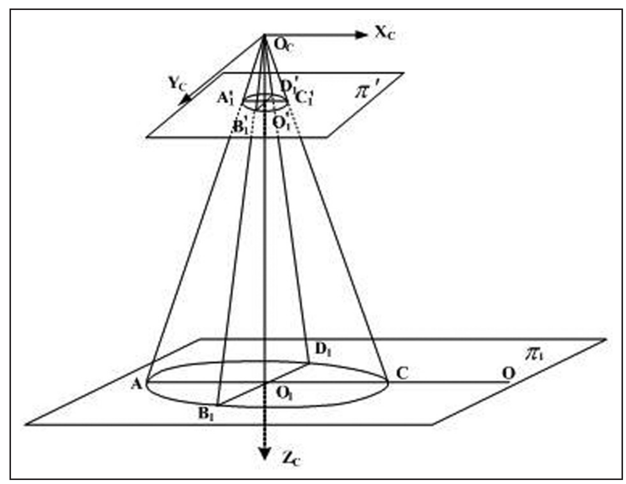

Figure 9 The perspective projection of the circular feature after the yaw motion.

Based on geometrical reasoning, this can be shown in Figure 10, which is simplified schematically. It mainly shows the two triangles ΔO_CBD and $\Delta O_CB_1D_1$. The angle between BD and B_1D_1 is the yaw angle ψ, as shown in Figure 10. Drawing the vertical lines from the point B_1 and D_1 to the segment O_CO_1, the foot points are E on the segment O_CO_1 and F on the extended line of the segment O_CO_1. In Figure 10, the length of the segment O_CO' is also called the effective focal length. Let f_0 be the effective focal length and r be the radius of the circle O_1. The distance between the optic centre O_C and the circle centre O_1 is l.

Based on the principle of similar triangles, the following equations can be obtained.

$$\begin{cases} \frac{B'_1O'}{B_1E} = \frac{O_cO'}{O_cE} \\ \frac{D'_1O'}{D_1F} = \frac{O_cO'}{O_cF} \end{cases} \tag{7}$$

where $B_1E = D_1F = r\cos\psi$. r is the radius of the circle and ψ is the yaw angle.

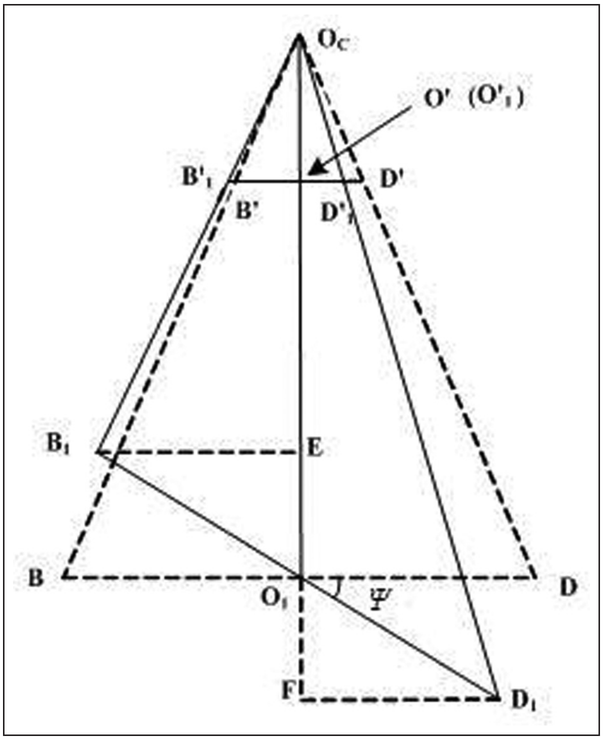

Figure 10 The simplified schematic representation of Figure 9.

Based on Equation (7), the following equations can be obtained by division.

$$\frac{B_1'O'}{D_1'O'} = \frac{O_cF}{O_cE} = \frac{l + r\sin\psi}{l - r\sin\psi} \tag{8}$$

where $B_1'O'$ and D_1O' are the two segments of an axis of image ellipse. Here we can let $b_1 = B_1'O'$ and $b_2 = D_1'O'$. l is the distance between the optic centre OC and the circle centre O1. r is the radius of the circle. Thus, Equation (8) can be expressed as

$$\frac{b_1}{b_2} = \frac{l + r\sin\psi}{l - r\sin\psi} \tag{9}$$

Based on Equation (9), we can finally obtain the equation of the yaw angle.

$$\psi = \arcsin\frac{(b_1 - b_2)l}{(b_1 + b_2)r} \tag{10}$$

In Equation (10), b_1 and b_2 are the two segments of the minor axis of the image ellipse. The values of b_1 and b_2 can be estimated from the acquired image. The values of l and r can be measured on the scene. If the values of yaw angles increase, the direction of the yaw motion is positive.

Computation methods of angles of pitch, roll and yaw in complex situations

In complex situations, the circular feature does two or three types of rotational motion at the same time. The circular feature's rotational motion can be decomposed of three kinds of rotation motion. So we can analyse the circular feature's rotational motion by computing the three kinds of rotational angles. Different from the method for computing pure pitch, roll and roll angles, we should select other appropriate tracking object, which can be used to compute rotational angles more easily.

In most situations, the object's rotational angles are relatively small. So in this section, we also consider $\pm 90°$ a measurement scope of the three types of rotational angles.

Another method for computing roll angle

In this section, we propose a new method for computing the roll angle of the circle. Different from in the Roll angle section above, we use the diameter AC as the tracking object, which is on the Z-axis initially, as shown in Figure 4. The reason is that the image of diameter AC is more stable than the diameter BD for our computations during the complex rotational motion.

From the Figure 5, we can see that the segment AC is parallel with its projection A′C′ in the image plane. When the circle O_1 rotates about the point O in the plane π, the two segments always keep parallel. The simplified image of the circle O_1 can be shown in Figure 11. Obviously, we can obtain the method for computing roll angle ϕ by measuring the slope of the diameter A′C′.

$$\phi = \begin{cases} \arctan k_{AC} + \pi/2, (k_{AC} < 0) \\ \arctan k_{AC} - \pi/2, (k_{AC} > 0) \\ 0, (k_{AC} = \infty) \end{cases} \tag{11}$$

where k_{AC} is the slope of A′C′, which is the image of diameter AC. When the diameter A′C′ is still vertical, it means the roll angle is zero, but when k_{AC} is zero, there will be two solutions: 90° and −90°. It is not difficult to distinguish the two cases by

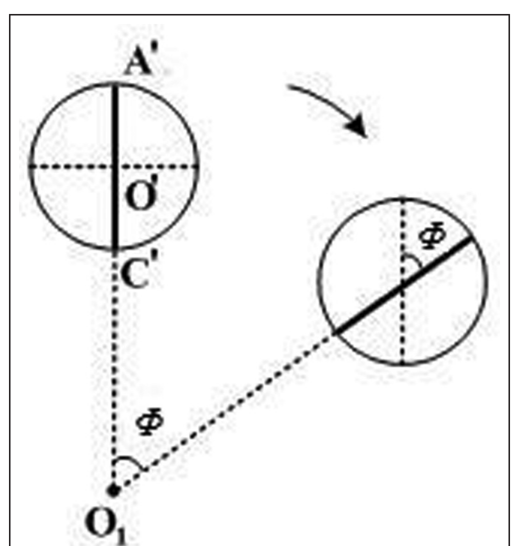

Figure 11 The image of the circle before and after the roll motion.

the images. For example, if the circle's image moves right relative to its initial position, it means the roll angle is negative.

Another method for computing pitch angle

In this section, we propose a new method to compute the pitch angle of the circular feature. Different from the Pitch angle section previously, we use the diameter AC as the tracking object, which is on the Z-axis initially, as shown in Figure 4.

Figure 12 is the simplified schematic representation of Figure 6. We draw three vertical lines from the point O_2, A_2 and C_2 to the segment O_CO_1, and the foot points are E, F and G separately. AC is the diameter in its initial status and A_2C_2 is the diameter after a pitch motion. $A'_2C'_2$ is the perspective projection of the diameter A_2C_2. The radius of the circle is r. The distance from O to O_1 is h. The distance from O_C to O_1 is l. The length of $O_CO'_1$ is the effective focal length f_0. The pitch angle in this process is θ, as shown in Figure 12.

We can obtain the following equations:

$$\begin{cases} \dfrac{A'_2O'_1}{A_2F} = \dfrac{O_CO'_1}{O_CF} \\ \dfrac{O'_1O'_2}{O_2E} = \dfrac{O_CO'_1}{O_CE} \\ \dfrac{O'_1C'_2}{C_2G} = \dfrac{O_CO'_1}{O_CG} \end{cases} \tag{12}$$

The derivation of the segment $A'_2O'_1$ is as follows:

$$O_1F = (h + r)\sin\theta$$

$$O_CF = O_CO_1 - O_1F = l - (h + r)\sin\theta$$

$$OD = h/\cos\theta$$

$$A_2D = OA_2 - OD = (h + r) - h/\cos\theta$$

$$A_2F = A_2D\cos\theta = (h + r)\cos\theta - h$$

We can obtain:

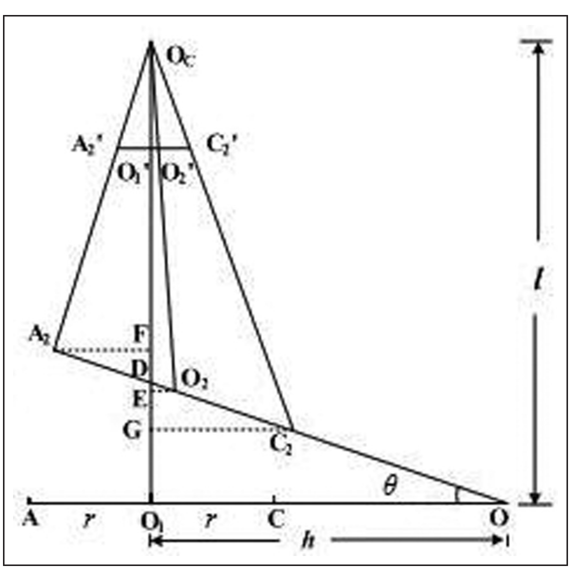

Figure 12 A new method for computing the pitch angle.

$$A'_2O'_1 = \frac{O_CO'_1 \cdot A_2F}{O_CF} = \frac{f_0[(h + r)\cos\theta - h]}{l - (h + r)\sin\theta} \tag{13}$$

The derivation of the segment $O'_1O'_2$ is as follows:

$$O_1E = h\sin\theta$$

$$O_1D = h\tan\theta$$

$$DE = O_1D - O_1E = h\tan\theta - h\sin\theta$$

$$O_2E = DE\cot\theta = h - h\cos\theta$$

$$O_CE = O_CO_1 - O_1E = l - h\sin\theta$$

So we can obtain:

$$O'_1O'_2 = \frac{O_CO'_1 \cdot O_2E}{O_CE} = \frac{f_0(h - h\cos\theta)}{l - h\sin\theta} \tag{14}$$

The derivation of the segment $O'_1C'_2$ is as follows:

$$O_1G = (h - r)\sin\theta$$

$$DG = O_1D - O_1G = h\tan\theta - (h - r)\sin\theta$$

$$C_2G = DG\cot\theta = h - (h - r)\cos\theta$$

$$O_CG = O_CO_1 - O_1G = l - (h - r)\sin\theta$$

So we can obtain:

$$O'_1C'_2 = \frac{O_CO'_1 \cdot C_2G}{O_CG} = \frac{f_0[h - (h - r)\cos\theta]}{l - (h - r)\sin\theta} \tag{15}$$

The circle O_1 can be imaged an ellipse and we can obtain the image of the diameter AC, the segment $A'_2C'_2$, which is composed of two segments, $A'_2O'_2$ and $O'_2C'_2$. Based on the Equations (13), (14) and (15), we can obtain:

$$\frac{A'_2O'_2}{O'_2C'_2} = \frac{A'_2O'_1 + O'_1O'_2}{O'_1C'_2 - O'_1O'_2} = \frac{\dfrac{f_0[(h + r)\cos\theta - h]}{l - (h + r)\sin\theta} + \dfrac{f_0(h - h\cos\theta)}{l - h\sin\theta}}{\dfrac{f_0[h - (h - r)\cos\theta]}{l - (h - r)\sin\theta} - \dfrac{f_0(h - h\cos\theta)}{l - h\sin\theta}} = \frac{l - (h - r)\sin\theta}{l - (h + r)\sin\theta} \tag{16}$$

Let a_1 and a_2 be the lengths of the segments $A'_2O'_2$ and $O'_2C'_2$. So,

$$\frac{a_1}{a_2} = \frac{l - (h - r)\sin\theta}{l - (h + r)\sin\theta} \tag{17}$$

$$\theta = \arcsin\frac{(a_1 - a_2)l}{(a_1 - a_2)h + (a_1 + a_2)r} \tag{18}$$

We can compute the pitch angle θ by Equation (18) in a complex situation. In this equation, a_1 and a_2, which are the lengths of images of two radii (A_2O_2 and O_2C_2, shown in Figure 12), can be measured from the acquired image. r is the radius of the circle. h is the distance from the circle centre O_1 to the origin O of the O–XYZ co-ordinate frame. l is the distance from the camera optical centre O_C to the circle centre O_1.

Another method for computing yaw angle

In the measurement of the three types of rotational angles, the measurement of the yaw angle is the most difficult and complex. In the Yaw angle section previously, we have proposed a method for computing the pure yaw angle through the image of diameter BD. In complex situation, the values of b_1 and b_2 (Equation 10) will change a lot and it is not suitable for the computation of yaw angle in complex situations. We should find a new method for computing the yaw angle, especially in the premise of a pitch motion.

We let the circle rotate about the Y-axis firstly and the pitch angle is θ. Then the circle rotates about the Z' axis (the body-fixed axis: a body-fixed co-ordinate frame is used and it can rotate along with the circle's rotational motion), as shown in Figure 13.

When the circle rotates about the Z' axis, the diameter B_2D_2 will perform the motion in the plane that B_2D_2 lies on and the Z' axis is perpendicular to. Let the plane be π_3, as shown in Figure 14. The diameter B_2D_2 rotates to B_3D_3 after a yaw motion. π'_3 is a vertical plane, which is parallel to the camera's image plane. $B'_2D'_2$ and $B'_3D'_3$ are the diameter's projections in the plane π'_3 (here we use parallel projection). Because plane π'_3 is parallel to the image plane, the image of the diameter B_2D_2 is parallel to the $B'_2D'_2$. Initially the slope of B_2D_2 and $B'_2D'_2$ is zero.

In Figure 14, $D_3H \perp B_2D_2$ and $D'_3H' \perp B'_2D'_2$. From the right figure in Figure 14, we can obtain the relation between D_3H and D'_3H'.

$$D'_3H' = D_3H \sin\theta \tag{19}$$

So,

$$\tan\psi' = \tan\psi \sin\theta \tag{20}$$

where ψ is the yaw angle and ψ' is the projection of the angle ψ in the plane π'_3. So,

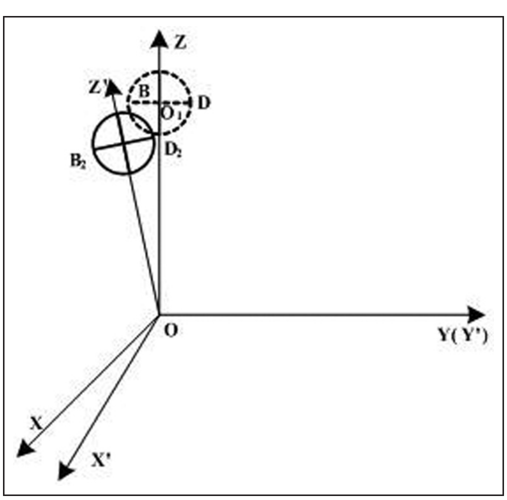

Figure 13 The schematic of the circle's pitch motion.

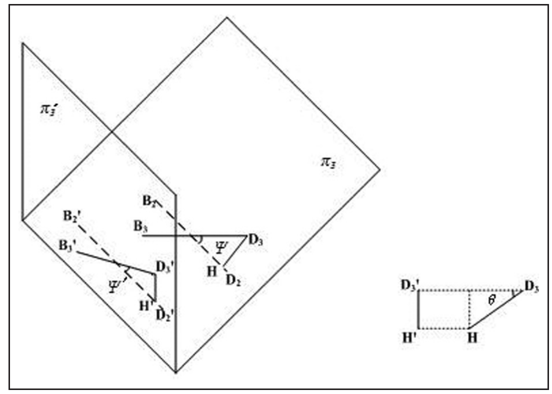

Figure 14 Analysis of the diameter in the yaw motion.

$$\psi = \arctan\frac{\tan\psi'}{\sin\theta} = \arctan\frac{k_{BD}}{\sin\theta} \tag{21}$$

Here θ is the pitch angle and $\theta \neq 0$. k_{BD} is the slope of the $B'_3D'_3$ and also the slope of the image of B_3D_3 in the camera's image plane.

If the circle also rotates about the X-axis and the roll angle is ϕ, the equation of yaw angle should be revised.

$$\psi = \arctan\frac{\tan(\arctan k_{BD} + \phi)}{\sin\theta} \tag{22}$$

If there are only the roll motion and yaw motion, the pitch angle θ in Equation (22) is zero. So the equation for computing the yaw angle should also be revised. In this situation, we can use the method proposed in the Yaw angle section above.

$$\psi = \arcsin\frac{(b_1 - b_2)l}{(b_1 + b_2)r} \tag{23}$$

Here b_1 and b_2 are the lengths of the images of two radii (BO_1 and DO_1, shown in Figure 13). The distance between the optic centre O_C and the circle centre O_1 is l. The radius of the circle is r.

So the computing method for yaw angle can be classified in two cases according to whether the circle performs the pitch motion.

$$\psi = \begin{cases} \arctan\dfrac{\tan(\arctan k_{BD} + \phi)}{\sin\theta}, (\theta \neq 0) \\ \arcsin\dfrac{(b_1 - b_2)l}{(b_1 + b_2)r}, (\theta = 0) \end{cases} \tag{24}$$

Method for measuring the pitch, roll and yaw angles in actual situations

In actual operation of the angles measurement, we can draw two diameters on the circular object. As shown in Figure 15, we can draw a solid line and a dotted line in the positions of AC and BD separately. The method mainly includes the following steps:

- ***Step 1:*** Take the image of the circle.
- ***Step 2:*** Image processing. We can obtain more distinguishable images, which contain the two diameters by

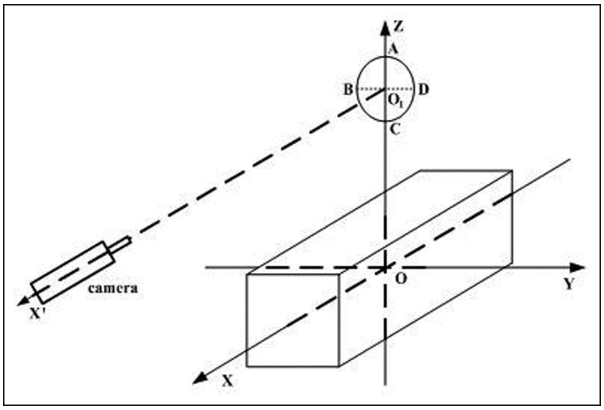

Figure 15 The schematic of measuring the angles of pitch, roll and yaw in complex situations.

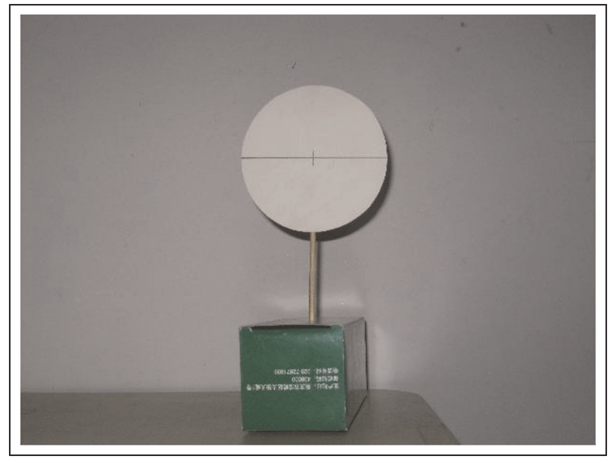

Figure 16 A box with a circular feature in the experiment.

some image processing algorithms, such as image denoising, image enhancement and morphological processing.

- ***Step 3:*** Compute the roll angle. If the diameter AC (the solid line) remains vertical, it means that there is no roll motion and the roll angle is zero. Otherwise, based on the method proposed previously, we can compute the roll angle of the circle by measuring the slope of the image of diameter AC (the solid line).
- ***Step 4:*** Compute the pitch angle. If the images of two radii in the diameter AC (the solid line) are equal in length, it means that there is no pitch motion and the pitch angle is zero. Otherwise, based on the second method proposed for computing the pitch angle, we can compute the pitch angle of the circle by measuring the images of two radii AO_1 and O_1C (the solid line).
- ***Step 5:*** Compute the yaw angle. If the images of two radii BO_1 and O_1D (the dotted line) are equal in length, it means there is no yaw motion and the yaw angle is zero. Otherwise, based on the second method proposed for computing yaw angle, we can compute the yaw angle of the circle by the measuring the slope of the image of diameter BD or the lengths of the images of two radii BO_1 and O_1D. This is an approximate angle measurement method in the complex situation.

Experiments and results

We have already analysed the object's three types of rotational motion with the help of a circular feature and proposed the method for computing the pitch, roll and yaw angles based on the principle of perspective projection in two situations. In order to verify the theoretical analysis and computational method for rotation angles that we proposed in this paper, some experiments were carried out as follows.

Measurement of the pure pitch, roll and yaw angles

As shown in Figure 16, there is a box on which a circular feature was fixed. In order to measure the rotational angles of a circular feature by the method of imaging analysis, it would be better to know the mode of the rotational motion. We set the camera as in Figure 4. In this study, we used a USB camera. The radius of the circular feature is 0.045 m and the distance between the optical centre of the camera and the plane of the circular feature is 0.6 m in this experiment. The distance between the circle centre and the object centre is 0.12 m.

We acquired the images of the circular feature during the three types of rotational motion. Each image is acquired when the circular feature rotates to some angles. So the actual rotational angel of each image is known. Figure 17 shows some images of the circular feature when it is in the different orientations. Then we analyse these images by image processing methods, such as decreasing noises, contrast enhancement and extraction of central line. The software used in this paper is Matlab. Finally, we can compute the values of rotational angles based on the method proposed previously. The results are shown in Figures 18, 19 and 20 separately. In each figure, the horizontal co-ordinates represent the actual values of angles and the vertical co-ordinates represent the measured values of angles. From the three figures, we can conclude that the approach proposed in this paper achieved good performance in spite of measurement errors.

Measurement of the pitch, roll and yaw angles in complex situations

When measuring the pitch, roll and yaw angles in complex situations, a holder is used to fix the circular feature. The circle can rotate about three vertical directions (X-axis, Y-axis and Z-axis) in the holder, as shown in Figure 21. The angles about each axis generated in the rotation can be obtained before the angle measurement. Then we use the camera to obtain the images of the circular feature in different orientations. The camera can be placed as shown in Figure 21. Here we use a USB camera and a circular plate, which is labelled with two diameters. The radius of the circular plate is 0.045 m and the initial distance between the optical centre of the camera and the plane of the circular plate is 0.6 m. The distance between the circle centre and the rotation centre is 0.28 m.

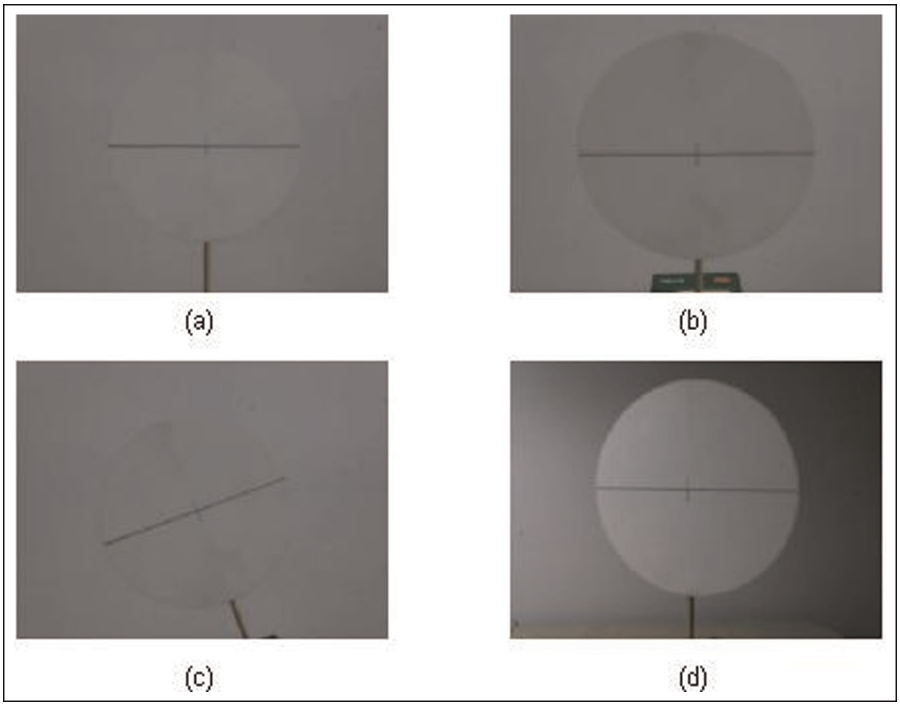

Figure 17 The circular feature's images in different status: (a) the image in the initial and static status; (b) the image during the pitch motion; (c) the image during the roll motion; (d) the image during the yaw motion.

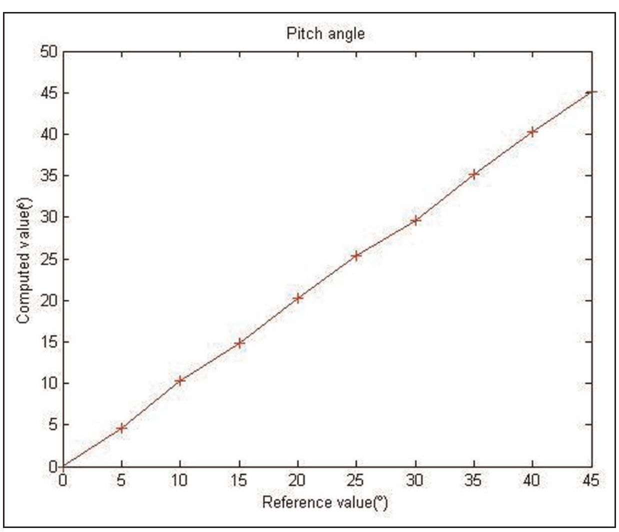

Figure 18 Measurement result for pitch angle.

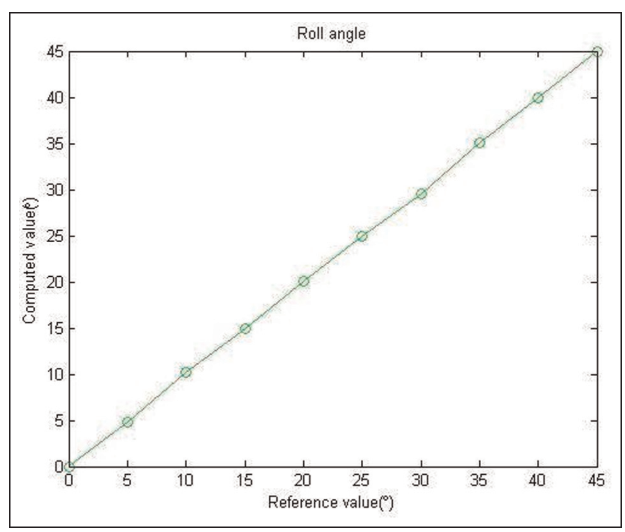

Figure 19 Measurement result for roll angle.

Through analysing the images of two diameters, we can compute the pitch, roll and yaw angles by the method proposed for measuring the pitch, roll and yaw angles in actual situations. The two diameters can be distinguished by the lines, i.e. the solid line and the dotted line.

We have captured images of the circular feature in different orientations and some are shown in Figure 22. Figure 22(a) displays the image of the circular feature in its initial state. We can find that the solid line diameter is vertical and the four radii of the two diameters (the solid line and the dotted line) are equal separately. So the three angles are all zero by our method proposed. We can also take the image of Figure 21(e) as an example. The circular feature's rotational angles relative to its initial status are: $-30°$ (roll angle), $35°$ (pitch angle) and $0°$ (yaw angle). The three angles are set in advance. Firstly, we compute the roll angle by computing the

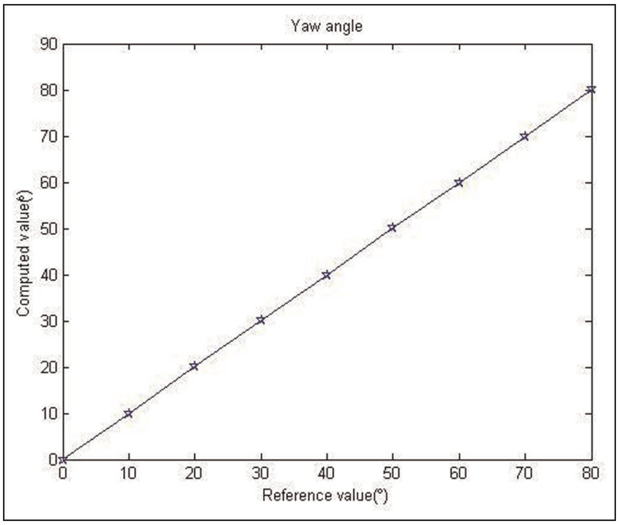

Figure 20 Measurement result for yaw angle.

Figure 21 The set-up in the experiment for measuring the three types of rotational angles.

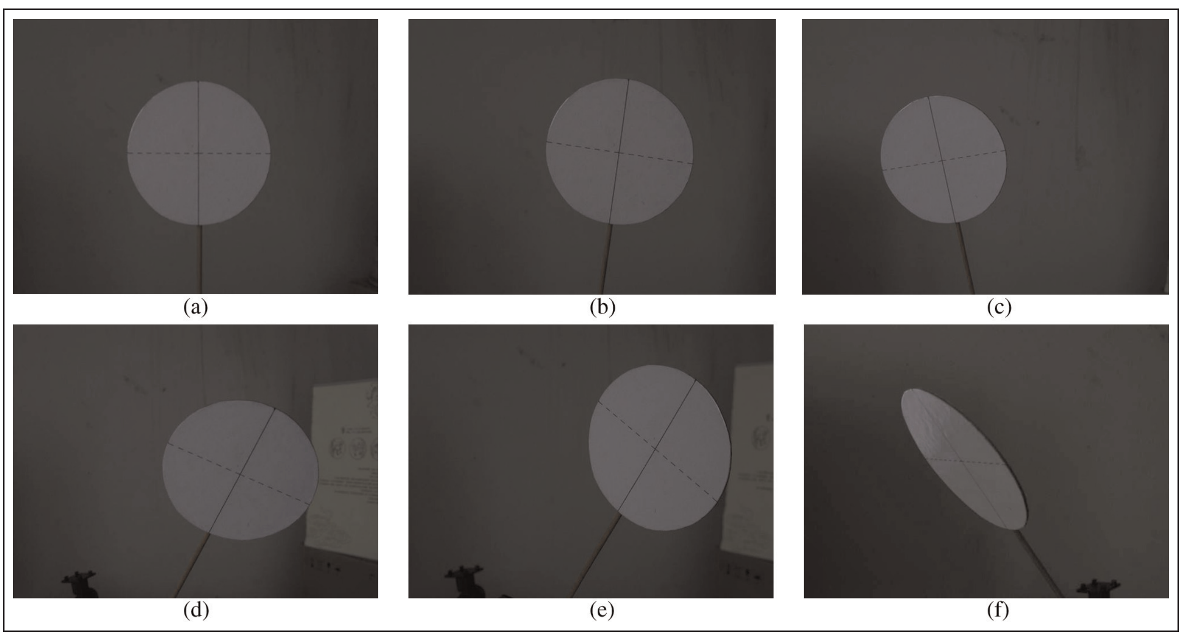

Figure 22 The circular feature's images in different orientations.

slope of the solid line diameter. The computed roll angle is −30.54°. Then we compute the pitch angle by measuring the lengths of two radii (the solid line). The computed pitch angle is 34.73°. At last, we compute the yaw angle. We find that the lengths of two radii (the dotted line) are equal. So the computed yaw angle is 0°. The detailed computation values of three angles are shown in Table 1.

Discussion

Error analysis

We have measured the three types of rotation angles based on the methods proposed in previously. Through the measurement results, we find that the computation methods of the pure pitch, roll and yaw angles are simple relative to the angles computation methods in complex situation. From Figures 18, 19 and 20, we can see that the methods of computing pure pitch, roll and yaw angles have achieved good effect. The error distribution can be shown in Figure 23. The maximum value of the absolutely error is 0.4°. From the data of the computed angles, we can compute the mean values of these errors. They are: 0.061° (pitch angle), −0.031° (roll angle) and 0.021° (yaw angle). The precision can meet a common need in actual applications.

In complex situations, there are two or three types of rotational motion at the same time. From Table 1, we can see that the computed roll and yaw angles have higher precision while

Table 1. The computed values of three angles in complex situations.

No.	Referenced values			Computed values		
	Roll angle	Pitch angle	Yaw angle	Roll angle	Pitch angle	Yaw angle
(a)	0°	0°	0°	0°	0°	0°
(b)	−8°	14°	0°	−7.61°	14.03°	0°
(c)	12°	28°	38°	12.31°	27.83°	39.7°
(d)	−28°	30°	−10°	−28.26°	30.9°	−8.25°
(e)	−30°	35°	0°	−30.54°	34.73°	0°
(f)	35°	25°	32°	34.23°	24.42°	34.93°

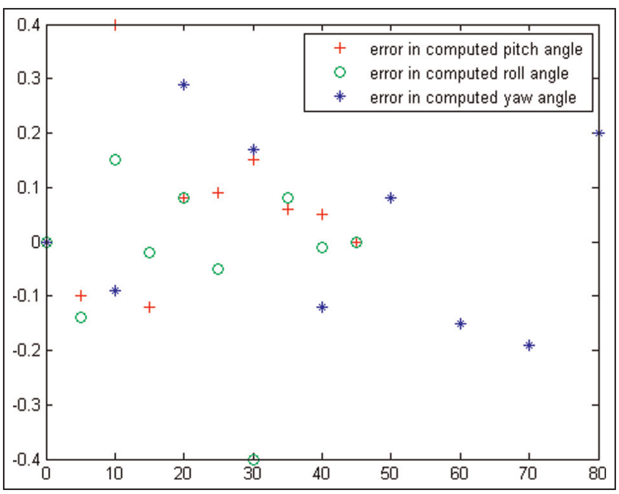

Figure 23 Error distributions in pure pitch, roll and yaw angles computation.

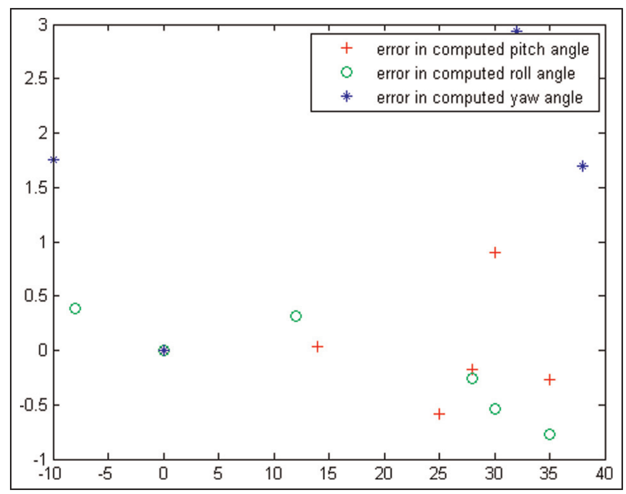

Figure 24 Error distributions in pitch, roll and yaw angle computation in complex situations.

the yaw angle has relatively lower precision. The error distribution is shown in Figure 24. The maximum value of the absolutely error is 2.93°. It occurs in the computation of yaw angle. From the data of computed angles, we can compute the mean values of these errors. They are: −0.015° (pitch angle), −0.145° (roll angle) and 1.063° (yaw angle). We can see that the computation methods in complex situations have lower precision than the computation methods of pure pitch, roll and yaw angles. The reason mainly is that the characteristics of the tracking objects (two diameters) will change in a complicated way during the motion. The computation method for yaw angle is an approximate method and is based on the computed values of pitch and roll angles. In this process, the error may increase. So the precision of yaw angle in complex situations is lowest, and the error shows an increasing tendency when the values of measured angles increase.

Other factors that impact the precision include: the lens distortion of the camera, including the pincushion distortion and the barrel distortion; the measurement error, including the error of the measurement values on the scene and the error of the measurement in the image; and the equipment error, including the installation error.

Comparison of two kinds of computation methods

The methods introduced for angles of pure pitch, roll and yaw can only solve the computation of the pure pitch, roll and yaw angles, but the methods introduced for angles of pitch, roll and yaw in complex situations not only can solve the computation of pitch, roll and yaw angles in complex situations, but solve the computation of the pure pitch, roll and yaw angles. So the methods introduced for angles of pitch, roll and yaw in complex situations have relevance in actual applications.

The values of some parameters used in the computation methods

In this paper, we should notice that there are three parameters: r (the radius of the circular feature), h (the distance between the circle centre and the object centre) and l (the distance between the optical centre of the camera and the circle centre in initial status), which should be set before the measurement. Here we only give the qualitative explanation about the values of the three parameters instead of the quantitative interpretation. The three parameters should be appropriate values in measuring the three types of rotation angles. They should be neither too big nor too small and they should meet our need for better imaging of the circular feature. For example, if the value of l is too big, the image of the circular feature will be much smaller and it will obviously have an impact on the computation precision. Otherwise, if the value of l is too small, the circular feature perhaps cannot be imaged completely. If the value of h is too big, a rotational motion with a small angle will cause the circular feature's large amplitude motion and it will have an impact on the imaging of the circular feature. If the value of h is too small, the object will hide the circular feature in some orientations. The three values are selected in many experiments by us.

The limitation of the methods proposed in this paper

The methods proposed in this paper have limitations. In this paper, we only consider that the rotational angle is in the scope of $\pm 90°$, but in some actual applications, such as head motion tracking or vehicle motion monitoring, the rotational angle is relatively small, so the methods can perform well, as we can see in the results we have acquired in the experiments.

Conclusions

In this paper, the object's three types of rotational motion – pitch, roll and yaw – were analysed based on a circular feature by the principle of perspective projection. First, we analysed the pure rotational motion of pitch, roll and yaw, and proposed the methods for computing the pure pitch, roll and yaw angles. Then we analysed the rotational motion in complex situations and proposed the different methods for computing the three angles in complex situations. Eventually, we performed experiments to verify the methods based on the analysis of this paper. Our results showed that the approach proposed in this paper could achieve good performance. Further work should be done to improve the measurement precision.

Acknowledgements

This work was supported by the National Natural Science Foundation of China (No. 10172043), International Science and Technology Cooperation Grant (No. BZ2010060) and Research Fund for the Doctoral Program of Higher Education of China (No. 20093218110024).

References

Ackerman JL, Proffit WR, Sarver DM, Ackerman MB and Kean MR (2007) Pitch, roll, and yaw: describing the spatial orientation of dentofacial traits. *American Journal of Orthodontics and Dentofacial Orthopedics* 131: 305–310.

Beaudot WHA and Mullen KT (2006) Orientation discrimination in human vision: psychophysics and modeling. *Vision Research* 46: 26–46.

Cosar S and Çetin M (2011) A graphical model based solution to the facial feature point tracking problem. *Image and Vision Computing* 29: 335–350.

Das SN and Das SK (2005) Mathematical model for coupled roll and yaw motions of a floating body in regular waves under resonant and non-resonant conditions. *Applied Mathematical Modelling* 29: 19–34.

Dornaika F and Sappa AD (2009) A featureless and stochastic approach to on-board stereo vision system pose. *Image and Vision Computing* 27: 1382–1393.

Ennos AE and Virdee MS (1982) High accuracy profile measurement of quasi-conical mirror surfaces by laser autocollimation. *Precision Engineering* 4: 5–8.

Fantoni C (2008) 3D surface orientation based on a novel representation of the orientation disparity field. *Vision Research* 48: 2509–2522.

Han J and Requicha AAG (1997) Integration of feature based design and feature recognition. *Computer-Aided Design* 29: 393–403.

Ji Q (2002) 3D Face pose estimation and tracking from a monocular camera. *Image and Vision Computing* 20: 499–511.

Kaiser A, Schultheiss TE, Wong JY, Smith DD, Han C, Vora NL, Pezner RD, Chen YJ and Radany EH (2006) Pitch, roll, and yaw variations in patient positioning. *International Journal of Radiation Oncology Biology Physics* 66: 949–955.

Kremmer M and Favier JF (2000) Calculating rotational motion in discrete element modelling of arbitrary shaped model objects. *Engineering Computations* 17: 703–714.

Kumar KD and Kumar K (1999) Satellite pitch and roll attitude maneuvers through very short tethers. *Acta Astronautica* 44: 257–265.

Lu Y and Leinonen T (2005) Solution and simulation of position-orientation for multi-spatial 3-RPS parallel mechanisms in series connection. *Multibody System Dynamics* 14: 47–60.

Ma SD (1993) Conics-based stereo, motion estimation, and pose determination. *International Journal of Computer Vision* 10: 7–25.

Price M and Morrison G (2009) Estimating 3D particle motion from high-speed video for simulation validation. *Engineering Computations* 26: 658–672.

Qiu Y and Griffin MJ (2005) Transmission of roll, pitch and yaw vibration to the backrest of a seat supported on a non-rigid car floor. *Journal of Sound and Vibration* 288: 1197–1222.

Regan D (1989) Orientation discrimination for objects defined by relative motion and objects defined by luminance contrast. *Vision Research* 29: 1389–1400.

Romero M and Bobick A (2004) Tracking head yaw by interpolation of template responses. *Proceedings of the 2004 Conference on Computer Vision and Pattern Recognition Workshop (CVPRW'04)* 5: 83.

Saito Y, Arai Y and Gao W (2009) Detection of three-axis angles by an optical sensor. *Sensors and Actuators A: Physical* 150: 175–183.

Salgado O, Altuzarra O, Viadero F and Hernández A (2010) Computational kinematics for robotic manipulators: instantaneous motion pattern. *Engineering Computations* 27: 495–518.

Sappa AD, Gerónimo D, Dornaika F and López A (2006) Real time vehicle pose using on-board stereo vision system. *International Conference on Image Analysis and Recognition, LNCS* 4142: 205–216.

Shang Y and Palmer PL (2011) Lunar lander's three-dimensional translation and yaw rotation motion estimation during a descent phase using optical navigation. *Acta Astronautica* 68: 149–159.

Shapiro LS and Brady JM (1992) Feature-based correspondence: an eigenvector approach. *Image and Vision Computing* 10: 283–288.

Tissainayagam P and Suter D (2005) Object tracking in image sequences using point features. *Pattern Recognition* 38: 105–113.

Triggs B (2004) Detecting keypoints with stable position, orientation, and scale under illumination changes. *Proceedings of the European Conference on Computer Vision IV* 3024: 100–113.

Zhu Z and Ji Q (2004) Real time 3D face pose tracking from an uncalibrated camera. *Proceedings of the 2004 Conference on Computer Vision and Pattern Recognition Workshop (CVPRW'04)* 5: 73.

Nomenclature

ϕ	Roll angle
θ	Pitch angle
ψ	Yaw angle
l	The distance between the optical centre of the camera and the circle centre in initial status
h	The distance between the circle centre and the origin of the O–XYZ co-ordinate frame
r	The radius of the circular feature
f_0	The effective focal length of the camera
a	The length of the image of diameter BD
k_{BD}	The slope of the image of diameter BD
k_{AC}	The slope of the image of diameter AC
a_1	The length of the image of radius AO_1 or A_2O_2 (after a pitch motion)
a_2	The length of the image of radius CO_1 or C_2O_2 (after a pitch motion)
b_1	The length of the image of radius BO_1 or B_1O_1 (after a yaw motion)
b_2	The length of the image of radius DO_1 or D_1O_1 (after a yaw motion)